JACS
JOURNAL OF THE AMERICAN CHEMICAL SOCIETY
Communication
pubs.acs.org/JACS

Poly(iohexol) Nanoparticles As Contrast Agents for in Vivo X-ray Computed Tomography Imaging

Qian Yin,[†] Felix Y. Yap,[‡] Lichen Yin,[†] Liang Ma,[†] Qin Zhou,[∥] Lawrence W. Dobrucki,[⊥] Timothy M. Fan,*[,§] Ron C. Gaba,*[,‡] and Jianjun Cheng*[,†]

[†]Department of Materials Science and Engineering, [§]Department of Veterinary Clinical Medicine, and [⊥]Department of Bioengineering, University of Illinois at Urbana−Champaign, Urbana, Illinois 61801, United States

[‡]Department of Radiology, University of Illinois at Chicago, Chicago, Illinois 60612, United States

[∥]Department of Pharmaceutical Science, Guangdong Pharmaceutical University, Guangzhou, Guangdong, China

Supporting Information

ABSTRACT: Biocompatible poly(iohexol) nanoparticles, prepared through cross-linking of iohexol and hexamethylene diisocyanate followed by coprecipitation of the resulting cross-linked polymer with mPEG-polylactide, were utilized as contrast agents for in vivo X-ray computed tomography (CT) imaging. Compared to conventional small-molecule contrast agents, poly(iohexol) nanoparticles exhibited substantially protracted retention within the tumor bed and a 36-fold increase in CT contrast 4 h post injection, which makes it possible to acquire CT images with improved diagnosis accuracy over a broad time frame without multiple administrations.

X-ray computed tomography (CT) is one of the most frequently used clinical diagnostic tools.[1] Current clinically used CT contrast agents are largely based on iodinated small molecules because of iodine's high X-ray absorption coefficient.[2] When used in vivo, however, the small-molecule contrast agents tend to be quickly eliminated from the circulation system and vascularized tissues because of their low molecular weights, large volume distributions, and fast renal clearance profiles.[3] Thus, the time window for CT imaging of the interested regions following administration of the small-molecule contrast agents is typically very narrow, beyond which the CT image would not have sufficient contrast and the regions of interest would be missed, resulting in under-representation of the number of metastatic lesions in a patient and incorrect evaluation of the extent of the disease. Recently, nanoparticles (NPs) have emerged as novel CT contrast agents, which overcome some of the drawbacks of iodinated small molecular contrast agents.[4] Several representative examples include iodinated liposomes,[5] polymer-coated bismuth sulfide nanoparticles (Bi_2S_3NP),[6] gold nanoparticles (GNP),[7] and organometallic molecule-based nanocolloids,[8] which have been reported to exhibit enhanced X-ray attenuation in vivo. Nevertheless, various issues remain to be addressed in these new contrast agents, including the challenge for the synthesis of iodolipid and unknown safety profiles of the inorganic NPs.

Polymeric NPs have recently emerged as promising contrast agents.[4a,9] Grafting iodinated small molecules to the pendant functional groups of hydrophilic polymers yields nanoparticulate contrast agents,[10] which however, often suffer from low loading efficiency and heterogeneous distribution of the iodinated small molecules.[11] When contrast agents are encapsulated in polymeric NPs, they can be homogenously distributed in the confined hydrophobic core and thus enable high X-ray attenuation.[12] However, undesired burst release of the encapsulated contrast agents from NPs upon exposure to the biological media complicates the image data analysis and thus prevents successful clinical applications.[1c] To address these challenges, we report here the development of poly(iohexol) NPs via cross-linking of iohexol with hexamethylene diisocyanate (HDI) followed by nanoprecipitation with mPEG-polylactide (mPEG-PLA). Such strategy takes advantage of the pharmacological and pharmacokinetic properties of NPs and effectively prevents the undesired leakage of the contrast agents. As such, substantially improved tissue retention and CT contrast were achieved using these NP contrast agents as apposed to free iohexol.

Clinically used iodinated contrast agents typically have multiple functional groups. Thus, we reasoned that a simple, straightforward strategy to make polymeric NP contrast agents with high molecular weight (MW) and high iodine loading would be cross-linking of these multifunctional contrast agents. The resulting cross-linked poly(contrast agent) would have very high X-ray absorption efficiency because of high-content iodinated residues that are homogeneously distributed and stably attached to the polymeric network. To demonstrate such hypothesis, we used iohexol, a widely used contrast agent with multiple hydroxyl groups as a comonomer to prepare poly(iohexol) upon cross-linking by HDI via the addition reaction (Figure 1A).

The reaction was mediated via dibutyltin dilaurate assisted O-acylation of HDI with the primary hydroxyl groups of iohexol (Figures 1A and S1). By changing the molar ratios of iohexol to HDI (I/H), a series of poly(iohexol)s (P1−P5) with different MWs were obtained (Figure S2A). GPC analysis revealed that P3 prepared at an I/H ratio of 1:3 had highest molecular weight (68.5 kDa), which is expected to have the lowest renal clearance rate.[13] The iodine loading of the final product was determined to be as high as 30.6%, close to the

Received: May 23, 2013
Published: August 29, 2013

 © 2013 American Chemical Society dx.doi.org/10.1021/ja405196f | J. Am. Chem. Soc. 2013, 135, 13620−13623

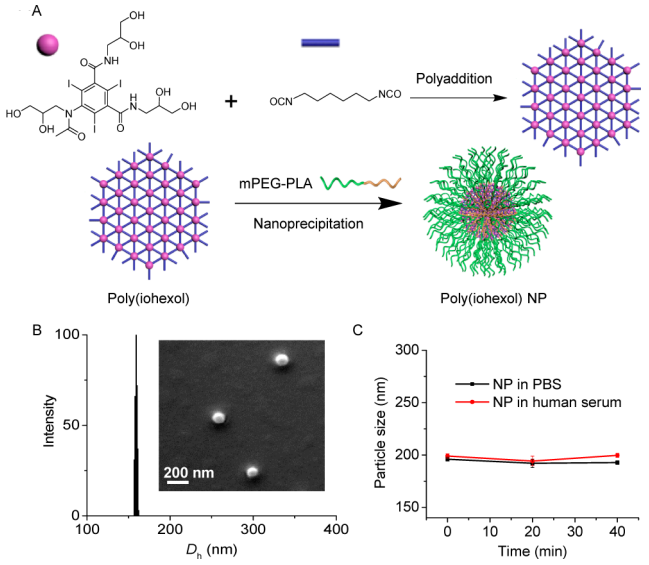

Figure 1. (A) Synthetic illustration of cross-linked poly(iohexol) and formulation of PEGylated poly(iohexol) NPs. (B) DLS analysis of NPs in water (0.5 mg/mL) and SEM image of NPs. (C) Stability of NPs following dilution with PBS (1×) or human serum (HS) buffer (HS/PBS = 1/1, v/v) for one-fold and further incubation at RT for different times.

calculated value based on the stoichiometric ratios of iohexol and HDI. Because poly(iohexol) is hydrophobic, we coprecipitated it with mPEG-PLA (PLA block of 1.4 kDa and mPEG segment of 5 kDa) to make PEGylated poly(iohexol) NPs, aiming to get NP contrast agents with PEG-coated surface and, as a result, to have minimal recognition by the reticuloendothelial systems,[14] negligible aggregation and protein binding,[15] and prolonged circulation.[16] The resulting NPs were ≈150 nm in diameter with narrow size distributions, as determined by dynamic light scattering (DLS) and SEM (Figure 1B). We analyzed the aqueous filtrate using HPLC and found that iohexol release was negligible, substantiating the design to stably conjugate iohexol to the polymer network via urethane linkages. As shown in Figures 1C and S4, the PEGylated poly(iohexol) NPs could prevent disassembly against dilutions upon administration and exhibited remarkable stability without any significant size changes or premature release of iohexol in PBS, human serum buffer, and cell culture medium for extended periods of time. We evaluated the X-ray absorption of poly(iohexol) NPs by acquiring images of a series of NP solutions with increased concentrations and subsequently converting them to Hounsfield maps for quantitative analysis. A linear correlation between NP concentration and the calculated CT attenuation (measured in Hounsfield units (HU), R^2 = 0.98) was observed (Figure S5A), demonstrating that poly(iohexol) NPs can function as contrast agents for quantitative CT studies.

We next evaluated the potential of poly(iohexol) NPs for in vivo CT diagnosis. A 20 mL poly(iohexol) NP solution mixed with 10 mL poppy seed oil was administered to New Zealand white rabbits by transarterial chemoembolization to enhance intratumoral deposition of NPs. The distribution of NPs was tracked by X-ray CT imaging. The cross-sectional imaging clearly revealed accumulation of NPs within liver parenchyma, evidenced by focal areas of high tissue attenuation (indicated by arrows, Figure S5B). Given this observation, these poly(iohexol) NPs could be potentially combined with a drug delivery system, offering extra benefits to visualize the accumulation of therapeutic agents within the hepatic tumor tissues noninvasively on CT scan and give the outcomes of administrated therapy.[17] Because a large number of the NPs distributed within portal vein and branches (see arrows pointed areas), high attenuation of these vascular structures could be observed (Figure S5B). This signal enhancement of vasculatures holds a great promise for the detection of the highly vascular hepatic metastasis.[15b]

We next performed a time course study by collecting a series of CT images at selected time intervals and evaluating the protracted retention of poly(iohexol) NPs as compared to free iohexol in the tumor bed in athymic nude mice bearing MCF-7 xenografts. Strong CT signals in the tumors were detected 5 min after intratumoral injection of iohexol to the control mice (Figure 2A), with enhanced density ΔHU obtained at the

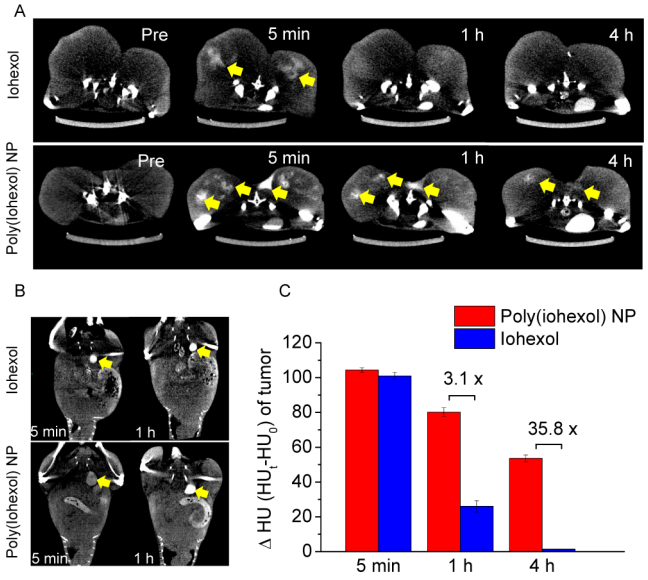

Figure 2. (A) Serial axial CT images of the MCF-7 tumors in mice following intratumoral injection of 200 μL of iohexol (upper panel) and poly(iohexol) NPs (lower panel) at 50 mg iohexol/kg. Images were taken before injection as well as 5 min, 1 h, and 4 h post injection. Arrows indicate the enhanced contrast regions in the tumor bed. (B) Serial sections of coronal CT images in MCF-7 xenografts bearing mice following the same treatment as described in (A). Arrows indicate the enhanced contrast regions in the bladder. (C) Enhanced density (ΔHU) of tumors at 5 min, 1 h, and 4 h after injection of poly(iohexol) NPs or iohexol.

scheduled time point subtracting that of untreated tumor tissues) of 101.0. However, the CT signal quickly decreased to 26.1 at 1 h postadministration (a 3.9-fold decrease) and became fairly weak and further decreased to 1.5 at 4 h postadministration (a 67.3-fold decrease from that of 5 min) and became nondetectable. In contrast, mice receiving poly(iohexol) NPs at equivalent doses of iohexol showed similar CT signal in the tumor (enhanced density ΔHU of 104.4) when CT image was collected 5 min after administration. As expected, protracted tumor tissue retention of the nanoparticulate contrast agent was observed. The enhanced density in tumor was 80.2 and 53.7 at 1 and 4 h postadministration, representing a decrease of CT signal intensity by only 23.2% and 48.6%, respectively, from that measured 5 min postadministration. The CT signal of the tumor bed of poly(iohexol) NPs treated mice was ∼36 times

dx.doi.org/10.1021/ja405196f | J. Am. Chem. Soc. 2013, 135, 13620−13623

higher than that of iohexol-treated mice 4 h postadministration. The protracted tumor tissue retention of poly(iohexol) NPs would also result in slower renal clearance. As shown in Figure 2B, the CT signal in the bladder was remarkably augmented immediately after administration of iohexol, and the high CT signal lasted for 1 h (Figure 2B), which accorded well with the fast renal clearance of small molecule contrast agents.[18] In comparison, poly(iohexol) NPs showed slower renal clearance; the CT signal in the bladder of the poly(iohexol) NP-treated mice was substantially weaker 5 min after administration (Figure 2B). These results therefore clearly demonstrated the benefit of using poly(iohexol) NPs over free iohexol for prolonged retention in the CT imaging of the region of interest. CT images at multiple time points can thus be acquired over a wide time window without the necessity of multiple contrast agent administrations, and more accurate representation of the metastatic lesions in the patients can also be ensured.

The protracted tumor retention of poly(iohexol) NP after intratumoral injection suggests that dynamic study with this new CT modality may be possible. We next performed preliminary fluoroscopic imaging study to evaluate the in vivo circulation and retention of poly(iohexol) NPs and iohexol when they were administered systemically. Imaging collection started at the same time with jugular vein injection of poly(iohexol) NPs or iohexol in C57BL/6 mice and continued for 1 h. As shown in Figure 3A, strong contrast in the bladder region was noticed immediately after jugular vein injection of iohexol to the control mice, and the contrast continued to increase drastically in the first 60 min. The contrasts in other soft tissues, such as heart, liver, and kidney substantially decreased within the first 60 min postadministration (Figure S6). In contrast, the bladder region of mice receiving poly(iohexol) NPs showed very weak contrast and stayed nondetectable, while the contrast in the heart, liver, and kidney showed negligible decrease in the first 60 min post administration (Figures 3A and S6). When administered intravenously, poly(iohexol) NPs exhibited much longer circulation half-life (15.9 h) compared to iohexol small molecule (3.8 h) (Figure 3B). These studies clearly showed the dramatically different renal and tissue clearance profiles of poly(iohexol) NPs and small molecule iohexol when used for in vivo imaging and suggest that poly(iohexol) NPs, compared with iohexol, may better serve to increase the temporal window for longer periods of imaging and data acquisition and allow more accurate disease diagnosis following intravenous contrast administration.

Safety profile is one of critical requirements for clinical translation.[19] To determine the safety of poly(iohexol) NPs, we first investigated their in vivo acute toxicity by histological assessment on major organs such as heart, liver, spleen, lung, kidney, and intestine, after intravenous administration of NPs in athymic nude mice at a high dose of poly(iohexol) NPs (up to 300 mg/kg). No mortality or obvious behavioral abnormalities were observed in any of the groups. In addition, no treatment related clinical signs and changes of body weights were noted. Representative sections of various organs taken 24 h after administrations were stained by hematoxylin and eosin (H&E) and evaluated by an independent pathologist (Figure S12). The absence of immune or inflammatory responses indicated low toxicity of the NPs. Besides the toxicity study, we also performed preliminary studies to evaluate the diodination with thyroid uptake and bioelimination of intravenously administered ^{64}Cu-labeled poly(iohexol) NPs in MCF-7

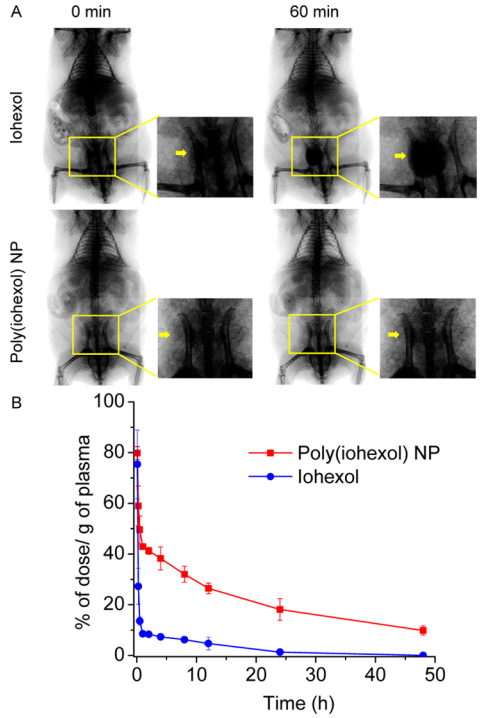

Figure 3. (A) Serial fluoroscopic images of C57BL/6 mice following jugular vein injection of 200 μL of conventional iodinated contrast agent (iohexol) solution (upper panel) and poly(iohexol) NP solution (lower panel) at 250 mg iohexol/kg, respectively. Images taken at 0 and 60 min after injection were shown. Arrows indicated the enhanced contrast in the bladder regions. (B) In vivo circulation time of poly(iohexol) NP and iohexol. ^{64}Cu-labeled poly(iohexol) NP and iohexol were injected intravenously through the tail vein of mice. At various time points (5, 15, and 30 min and 1, 2, 4, 6, 8, 12, 24, and 48 h), blood was withdrawn intraorbitally, and the radioactivity was measured by the γ-counter to evaluate the systemic circulation of the poly(iohexol) NP (red) and iohexol (blue) (n = 3).

tumor-bearing athymic nude mice (Figures S9 and S10). The accumulation of poly(iohexol) NPs in the thyroid was found to be 1.19% I.D./g 24 h post injection. With such a low uptake in the thyroid, poly(iohexol) NPs are unlikely to cause iodine-provoked hyperthyroidism, although the thyroid function of poly(iohexol) NPs treated mice needs to be further assessed. The accumulation of poly(iohexol) NPs in the bladder, urine and feces 24 h post injection were found to be 2.17%, 0.95%, and 11.36% I.D./g, respectively, demonstrating that the poly(iohexol) NPs can be eliminated from the body via urine and feces.

In conclusion, we designed and synthesized poly(iohexol) by using iohexol as a multifunctional monomer to mediate cross-linking polymerization. The resulting poly(iohexol) was coprecipitated with mPEG-PLA to form PEGylated poly-(iohexol) NPs as an in vivo applicable contrast nanoprobe. These NPs showed negligible toxicity, remarkable stability, and substantially improved protracted retention in the tumor bed, which makes it possible to acquire CT images over a wide time frame without multiple administrations and improves the diagnosis accuracy for the representation of the region of interest. Because degradable domains (e.g., ester bond) can be easily integrated to poly(iohexol) by selecting ester-containing bis-isocyanate as the comonomer, degradable poly(iohexol) can be developed to ensure complete renal clearance at the end of the study, which will be far superior to inorganic nano-

dx.doi.org/10.1021/ja405196f | J. Am. Chem. Soc. 2013, 135, 13620−13623

particulate contrast agents (e.g., GNPs) with unfavorable clearance profiles and long-term safety concerns. Given the simplicity of the synthesis and the fact that the poly(iohexol) NPs can be easily scaled up and formulated in solid form with well-preserved NP property with negligible aggregation (Figure S4B), we anticipate that the biocompatible poly(iohexol) NPs could potentially be used as CT imaging contrast agents in the clinic to improve diagnostic accuracy and patient compliance.

■ ASSOCIATED CONTENT

Supporting Information

Additional CT images and HU measurements, selected ^{1}H NMR, FT-IR, and ESI spectra of synthesized materials, GPC characterization of polymers, DLS analysis of particles, PET/CT imaging of in vivo biodistribution, ex vivo γ-counter analysis, and cytotoxicity and histopathology evaluation. This material is available free of charge via the Internet at http://pubs.acs.org.

■ AUTHOR INFORMATION

Corresponding Authors

jianjunc@illinois.edu
rongaba@yahoo.com
t-fan@illinois.edu

Notes

The authors declare no competing financial interest.

■ ACKNOWLEDGMENTS

This work is supported by Philips Healthcare/Radiological Society of North America Research Seed grant no. RSD1104, the National Institute of Health (Director's New Innovator Award 1DP2OD007246-01 and 1R21CA152627), and Morris Animal Foundation (D09CA-083). Q.Y. was funded at UIUC from the NIH National Cancer Institute Alliance for Nanotechnology in Cancer "Midwest Cancer Nanotechnology Training Center" grant R25 CA154015A.

■ REFERENCES

(1) (a) Weissleder, R. *Science* **2006**, *312*, 1168−1171. (b) Liu, Y. L.; Ai, K. L.; Liu, J. H.; Yuan, Q. H.; He, Y. Y.; Lu, L. H. *Angew. Chem., Int. Ed.* **2012**, *51*, 1437−1442. (c) Rutten, A.; Prokop, M. *Anti-Cancer Agents Med. Chem.* **2007**, *7*, 307−316. (d) Schenkman, L. *Science* **2011**, *331*, 1002−1004.

(2) (a) Dekrafft, K. E.; Xie, Z. G.; Cao, G. H.; Tran, S.; Ma, L. Q.; Zhou, O. Z.; Lin, W. B. *Angew. Chem., Int Ed.* **2009**, *48*, 9901−9904. (b) Hyafil, F.; Cornily, J. C.; Feig, J. E.; Gordon, R.; Vucic, E.; Amirbekian, V.; Fisher, E. A.; Fuster, V.; Feldman, L. J.; Fayad, Z. A. *Nat. Med.* **2007**, *13*, 636−641.

(3) Bae, K. T. *Radiology* **2010**, *256*, 32−61.

(4) (a) Liu, Y. L.; Ai, K. L.; Lu, L. H. *Acc. Chem. Res.* **2012**, *45*, 1817−1827. (b) Jakhmola, A.; Anton, N.; Vandamme, T. F. *Adv. Healthcare Mater* **2012**, *1*, 413−431. (c) Ai, K. L.; Liu, Y. L.; Liu, J. H.; Yuan, Q. H.; He, Y. Y.; Lu, L. H. *Adv. Mater.* **2011**, *23*, 4886−4891.

(5) Elrod, D. B.; Partha, R.; Danila, D.; Casscells, S. W.; Conyers, J. L. *J. Nanomed. Nanotechnol.* **2009**, *5*, 42−45.

(6) (a) Rabin, O.; Perez, J. M.; Grimm, J.; Wojtkiewicz, G.; Weissleder, R. *Nat. Mater.* **2006**, *5*, 118−122. (b) Pan, D.; Roessl, E.; Schlomka, J. P.; Caruthers, S. D.; Senpan, A.; Scott, M. J.; Allen, J. S.; Zhang, H. Y.; Hu, G.; Gaffney, P. J.; Choi, E. T.; Rasche, V.; Wickline, S. A.; Proksa, R.; Lanza, G. M. *Angew. Chem., Int. Ed.* **2010**, *49*, 9635−9639.

(7) (a) Popovtzer, R.; Agrawal, A.; Kotov, N. A.; Popovtzer, A.; Balter, J.; Carey, T. E.; Kopelman, R. *Nano Lett* **2008**, *8*, 4593−4596. (b) Reuveni, T.; Motiei, M.; Romman, Z.; Popovtzer, A.; Popovtzer, R. *Int. J. Nanomed.* **2011**, *6*, 2859−2864.

(8) (a) Pan, D. P. J.; Schirra, C. O.; Senpan, A.; Schmieder, A. H.; Stacy, A. J.; Roessl, E.; Thran, A.; Wickline, S. A.; Proska, R.; Lanza, G. M. *ACS Nano* **2012**, *6*, 3364−3370. (b) Pan, D.; Williams, T. A.; Senpan, A.; Allen, J. S.; Scott, M. J.; Gaffney, P. J.; Wickline, S. A.; Lanza, G. M. *J. Am. Chem. Soc.* **2009**, *131*, 15522−15527.

(9) (a) Lusic, H.; Grinstaff, M. W. *Chem. Rev.* **2013**, *113*, 1641−1666. (b) Lee, D.; Khaja, S.; Velasquez-Castano, J. C.; Dasari, M.; Sun, C.; Petros, J.; Taylor, W. R.; Murthy, N. *Nat. Mater.* **2007**, *6*, 765−769. (c) Shrestha, R.; Elsabahy, M.; Luehmann, H.; Samarajeewa, S.; Florez-Malaver, S.; Lee, N. S.; Welch, M. J.; Liu, Y. J.; Wooley, K. L. *J. Am. Chem. Soc.* **2012**, *134*, 17362−17365. (d) Lee, C. C.; Liu, Y. M.; Reineke, T. M. *ACS Macro Lett* **2012**, *1*, 1388−1392.

(10) (a) Kojima, C.; Umeda, Y.; Ogawa, M.; Harada, A.; Magata, Y.; Kono, K. *Nanotechnology* **2010**, *21*, 245104. (b) Mottu, F.; Rufenacht, D. A.; Laurent, A.; Doelker, E. *Biomaterials* **2002**, *23*, 121−131.

(11) Aillon, K. L.; El-Gendy, N.; Dennis, C.; Norenberg, J. P.; McDonald, J.; Berkland, C. *Mol. Pharmaceutics* **2010**, *7*, 1274−1282.

(12) (a) Kong, W. H.; Lee, W. J.; Cui, Z. Y.; Bae, K. H.; Park, T. G.; Kim, J. H.; Park, K.; Seo, S. W. *Biomaterials* **2007**, *28*, 5555−5561. (b) Sun, G. R.; Berezin, M. Y.; Fan, J. D.; Lee, H.; Ma, J.; Zhang, K.; Wooley, K. L.; Achilefu, S. *Nanoscale* **2010**, *2*, 548−558.

(13) Fox, M. E.; Szoka, F. C.; Frechet, J. M. J. *Acc. Chem. Res.* **2009**, *42*, 1141−1151.

(14) Amoozgar, Z.; Yeo, Y. *Wiley Interdiscip. Rev.: Nanomed. Nanobiotechnol.* **2012**, *4*, 219−233.

(15) (a) Langer, R. *Nature* **1998**, *392*, 5−10. (b) Kim, D.; Park, S.; Lee, J. H.; Jeong, Y. Y.; Jon, S. *J. Am. Chem. Soc.* **2007**, *129*, 7661−7665. (c) Cheng, J.; Teply, B. A.; Sherifi, I.; Sung, J.; Luther, G.; Gu, F. X.; Levy-Nissenbaum, E.; Radovic-Moreno, A. F.; Langer, R.; Farokhzad, O. C. *Biomaterials* **2007**, *28*, 869−876.

(16) (a) Tong, R.; Yala, L. D.; Fan, T. M.; Cheng, J. J. *Biomaterials* **2010**, *31*, 3043−3053. (b) Roberts, M. J.; Bentley, M. D.; Harris, J. M. *Adv. Drug Delivery Rev.* **2002**, *54*, 459−476.

(17) Murata, S.; Mine, T.; Ueda, T.; Nakazawa, K.; Onozawa, S.; Yasui, D.; Kumita, S. *Sci. World J.* **2013**, *2013*, 479805.

(18) Kirberger, R. M.; Cassel, N.; Carstens, A.; Goddard, A. *Acta Vet. Scand.* **2012**, *54*, 47.

(19) (a) Heath, J. R.; Davis, M. E. *Annu. Rev. Med.* **2008**, *59*, 251−265. (b) Tong, R.; Cheng, J. *Polym. Rev.* **2007**, *47*, 345−381.